Supporting Information

Highly Luminescent and Thermostable Lanthanide-carboxylate Framework Materials with Helical Configuration

Huabin Zhang, [†,‡] Liujiang Zhou, [†,‡] Jing Wei [†,‡] Zhihua Li[†], Ping Lin[†] and Shaowu-Du[*,†]

[†] *State Key Laboratory of Structural Chemistry, Fujian Institute of Research on the Structure of Matter, Chinese Academy of Sciences, Fuzhou, Fujian 350002, P. R. China.*

[‡] *Graduate University of Chinese Academy of Sciences, Beijing 100039, P. R. China.*

* Corresponding author, E-mail: swdu@fjirsm.ac.cn. Fax: 86-591-83709470.

Figure S1. XRPD patterns for the as-synthesized compounds **1–3** and the simulated patterns from single-crystal X-ray data.

Figure S2. TGA curves for compounds **2** and **3**.

Figure S3. As-synthesized patterns and variable-temperature PXRD patterns for **1** at elevated temperature**.**

Figure S4. The TG and DSC curves of calcinated samples of 1.

Figure S5. The IR spectra of as-synthesized and calcinated samples of 1.

Figure S6. The UV-vis absorbance spectra of compounds **1–3** in methanol.

Figure S7. Excitation and emission spectrum of compound **2** in 77 K.

Figure S8. Solid-state emission spectra for calcinated samples of **1** (a) and **3** (b) at room temperature.

Table S1. Pertinent Crystal Data and Structure Refinement Results for compounds 1–3.

Table S2. The details of the contributions of orbital transitions for some electronic transitions with large oscillator strengths for ligand from the TD-DFT calculation.

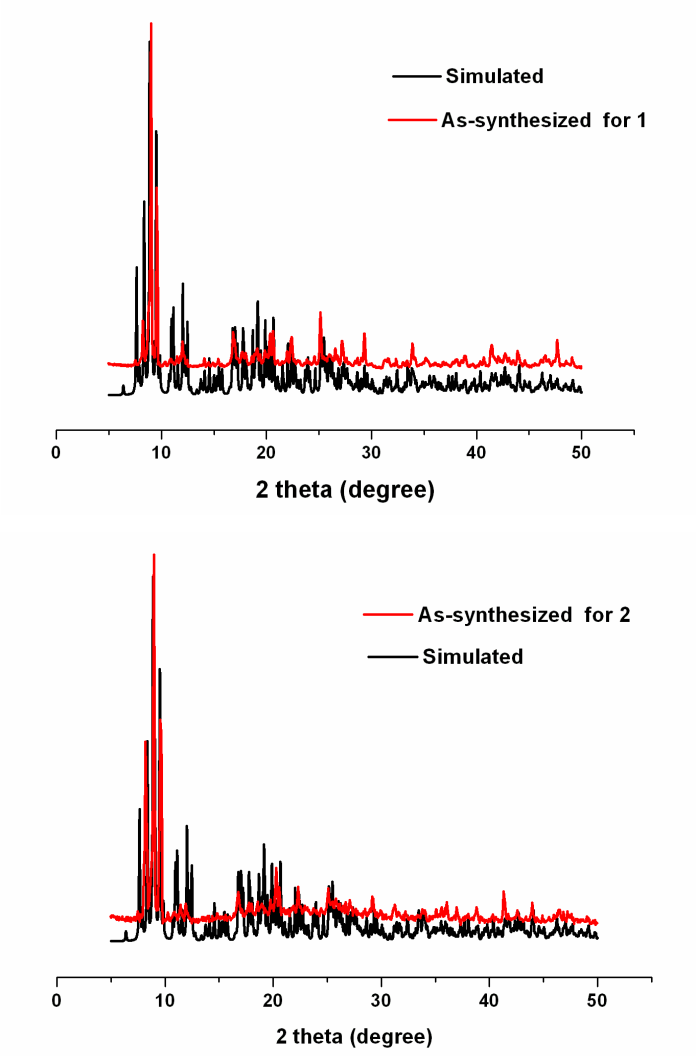

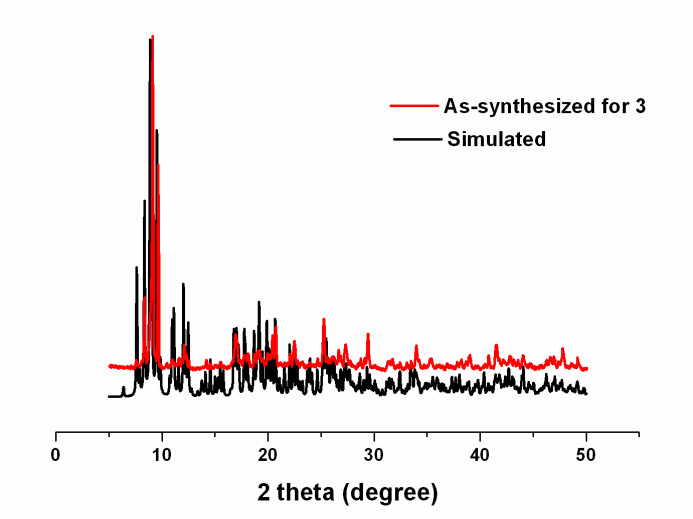

Figure S1. XRPD patterns for the as-synthesized compounds **1–3** and the simulated patterns from single-crystal X-ray data**.**

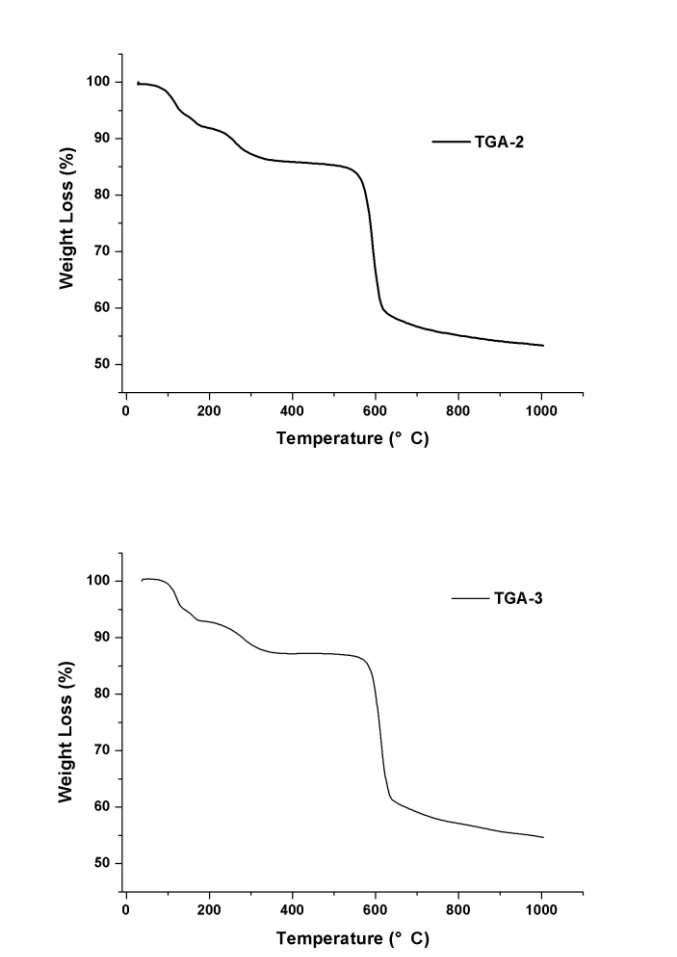

Figure S2. TGA curves for compounds **2** and **3.**

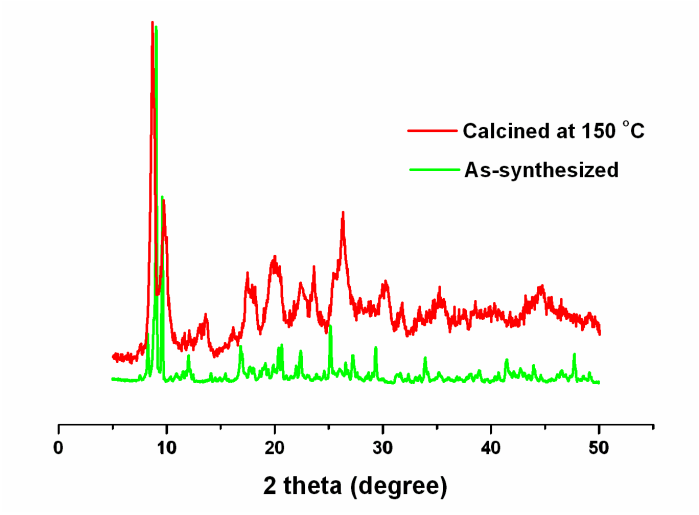

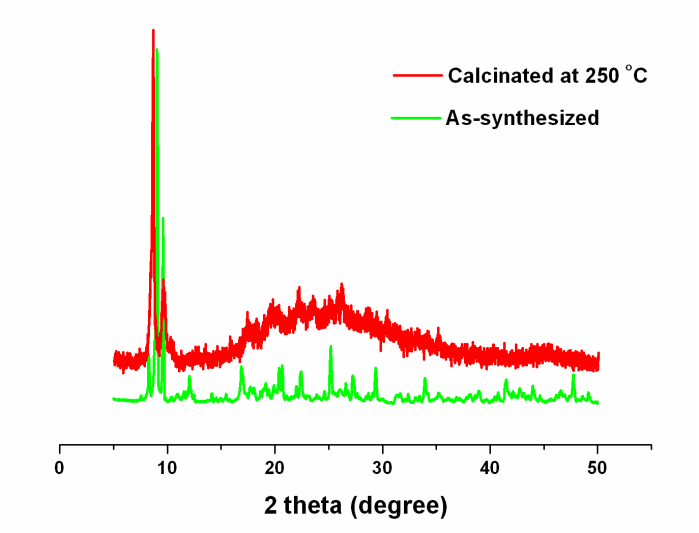

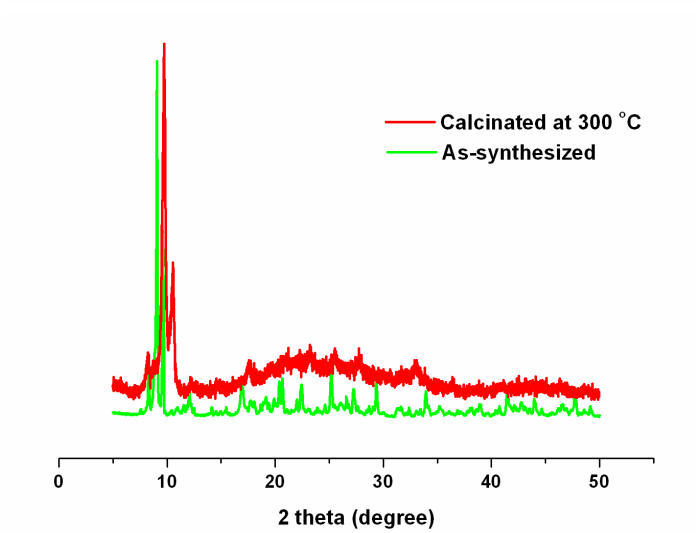

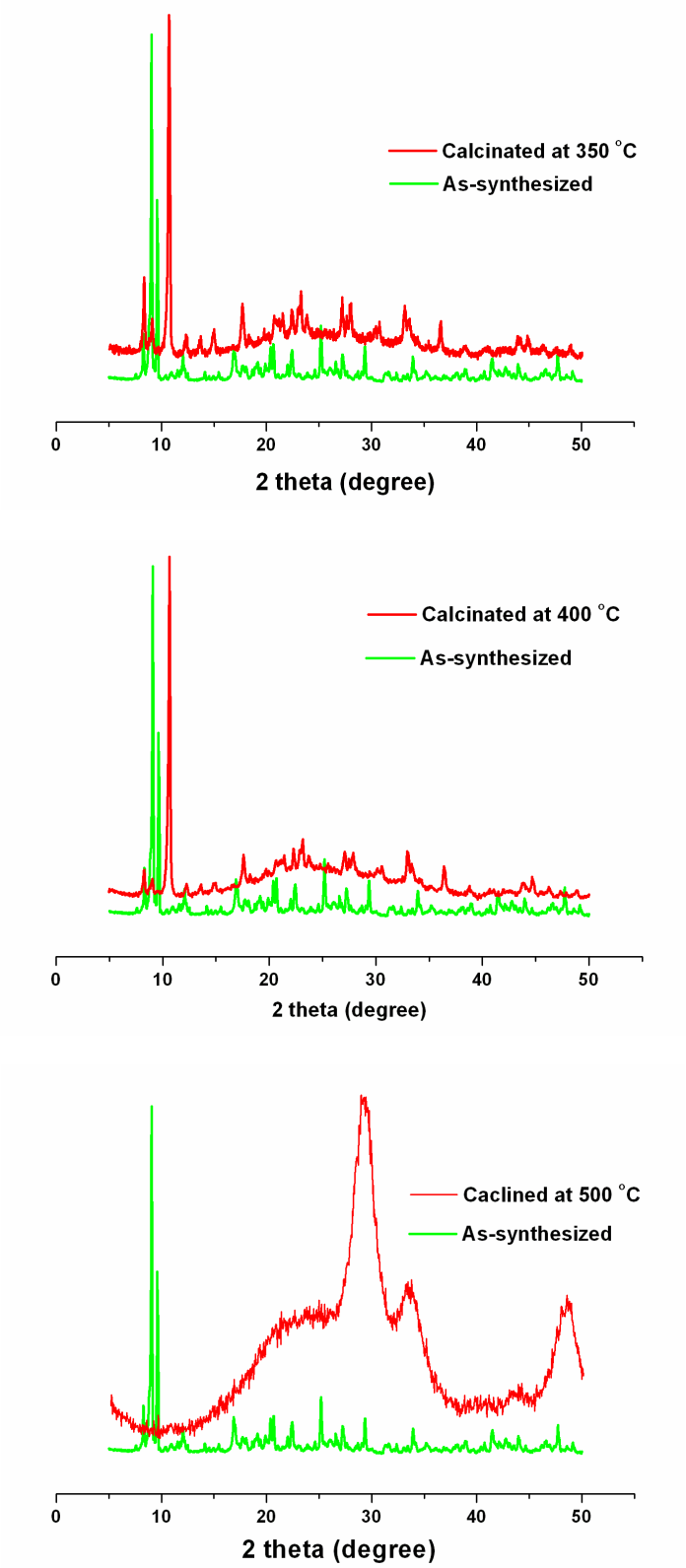

Figure S3. As-synthesized patterns and variable-temperature PXRD patterns for **1** at elevated temperature.

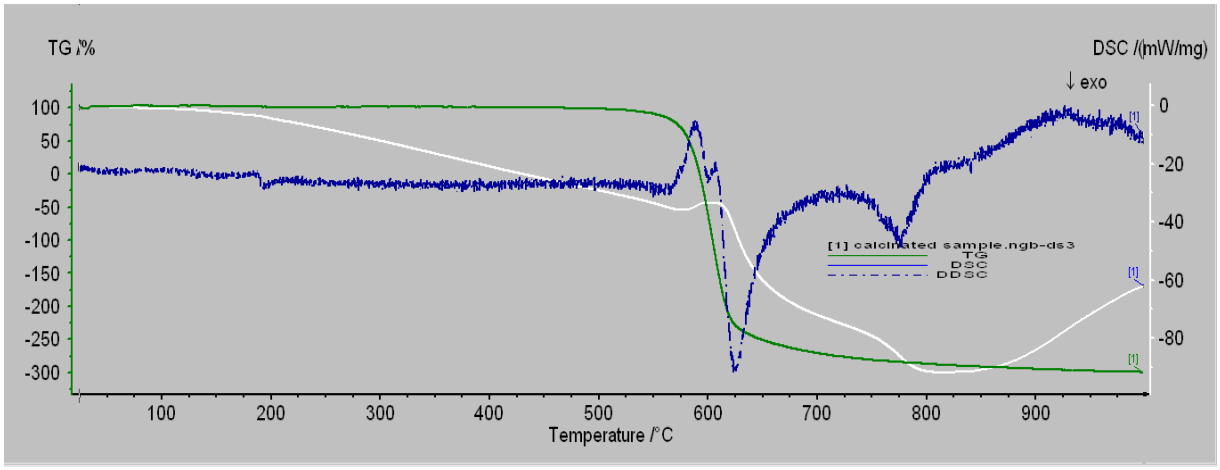

Figure S4. The TG and DSC curves of calcinated samples of **1**.

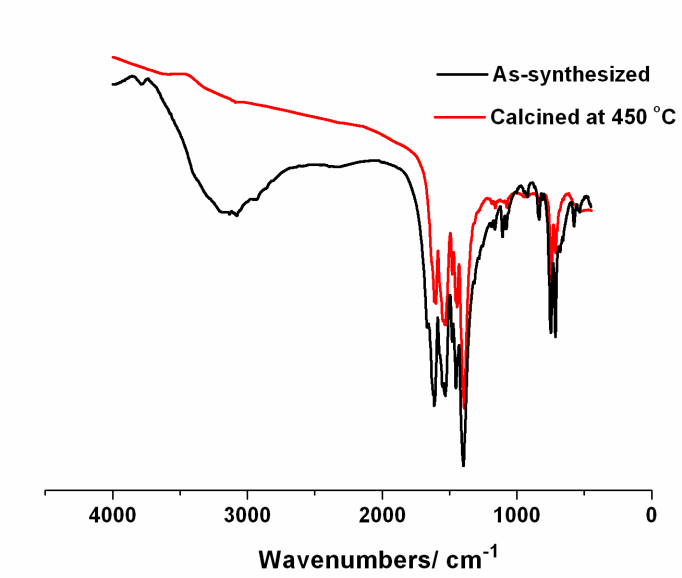

Figure S5. The IR spectra of as-synthesized and calcinated samples of **1**.

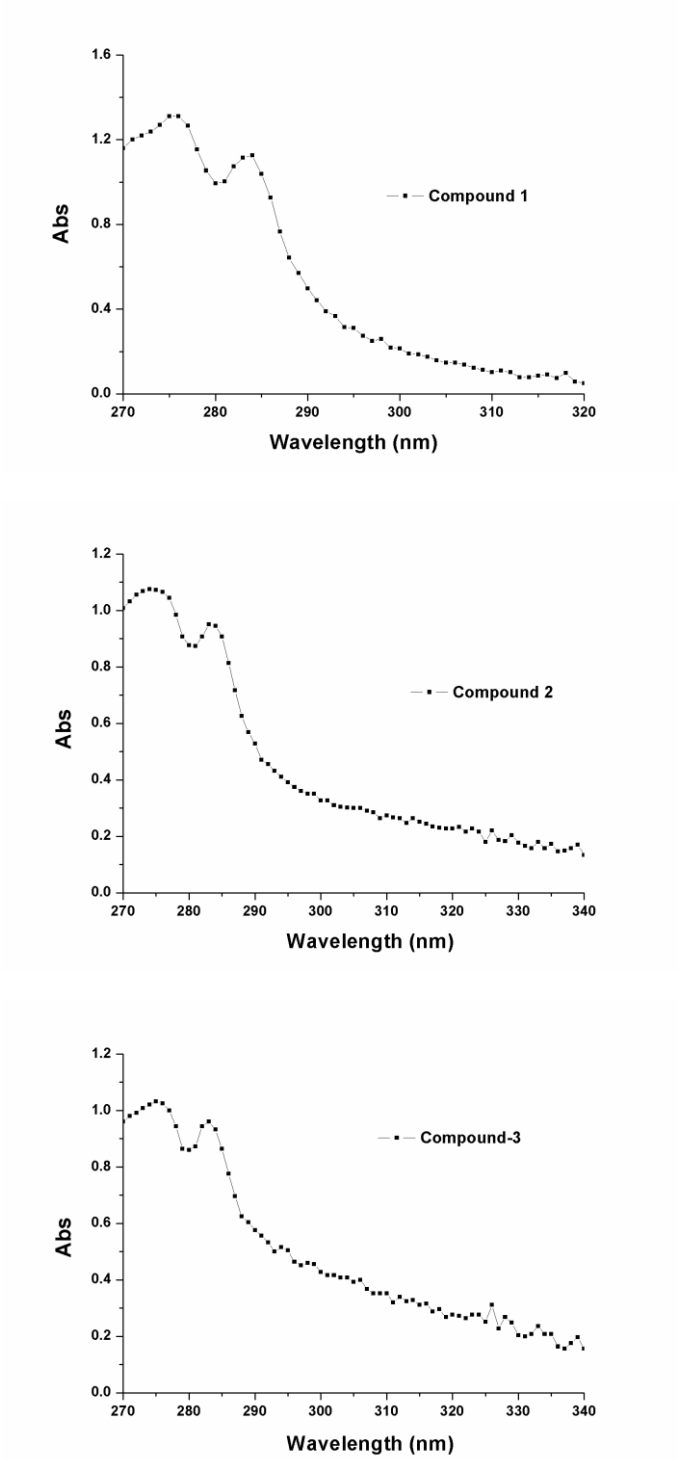

Figure S6. The UV-vis absorbance spectra of compounds **1–3** in methanol.

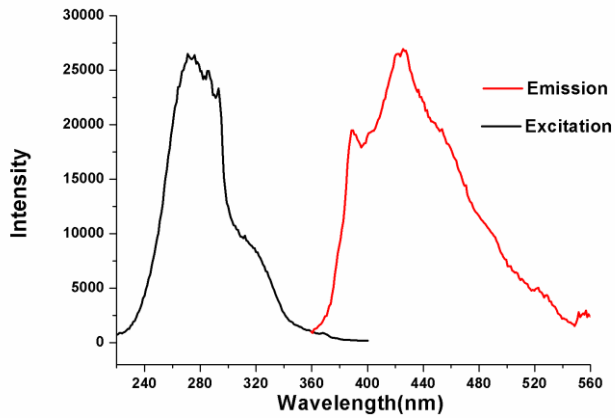

Figure. S7. Excitation and emission spectrum of compound **2** in 77 K.

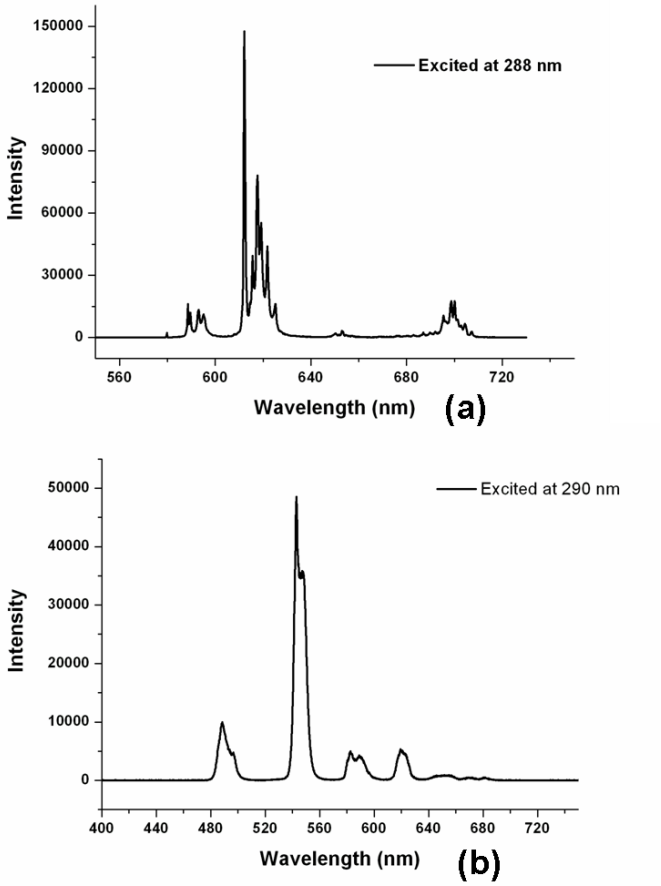

Fig. S8 Solid-state emission spectra for calcinated samples of **1** (a) and **3** (b) at room temperature.

Table S1. Pertinent Crystal Data and Structure Refinement Results for compounds **1–3**

Compounds	**1**	**2**	**3**

Formula	$C_{54}H_{45}N_2O_{32}Eu_4$	$C_{54}H_{45}N_2O_{32}Gd_4$	$C_{54}H_{45}N_2O_{32}Tb_4$
M (g mol^{-1})	1841.79	1862.93	1869.63
Crystal system	Triclinic	Triclinic	Triclinic
Space group	$P\bar{1}$	$P\bar{1}$	$P\bar{1}$
a (Å)	10.849(3)	10.836 (3)	10.850 (4)
b (Å)	14.172(5)	14.156 (4)	14.135 (5)
c (Å)	20.208(7)	20.139(2)	20.084 (7)
α(°)	86.734 (7)	86.706(5)	86.494(7)
β(°)	83.852 (9)	83.875(4)	83.743(6)
γ(°)	79.093 (7)	78.990 (4)	78.839 (8)
V (Å^3)	3031.2 (17)	3012.9 (14)	3001.4 (18)
Z	2	2	2
D_c (g cm^{-3})	2.016	2.048	2.063
□ μ (mm^{-1})	4.18	4.44	4.75
F(000)	1778	1468	1788
GOF	0.99	0.98	1.06
R_1[a]	0.038	0.0339	0.0404
	(0.0435)[b]	(0.0392)[b]	(0.0472)[b]
wR_2[a]	0.080	0.0834	0.1017
	(0.0820)[b]	(0.887)[b]	(0.1088)[b]

$R = \sum (||F_o| - |F_c||)/\sum |F_o|$, $wR = \{ \sum w[(F_o^2 - F_c^2)^2]/ \sum w[(F_o^2)^2]\}^{1/2}$; [$F_o > 4\sigma (F_o)$].

[b] Based on all data.

Table S2. The details of the contributions of orbital transitions for some electronic transitions with large oscillator strengths for ligand from the TD-DFT calculation.

Excited State 1:	Percentage (%)	Excitation energy (nm)	Oscillator strength
40 -> 45	15.99	261.87	0.0002
40 -> 46	2.45		
41 -> 44	77.74		

Excited State 2:	Percentage (%)	Excitation energy (nm)	Oscillator strength
42 -> 45	33.21	260.62	0.0175
43 -> 44	66.76		